Math. Num. Sin.
21:2(1999), 225–236.

Chinese J. Num. Math. & Appl.
21:3(1999), 69–82.

A SECOND-ORDER GODUNOV METHOD FOR COMPUTING WAVE AND FRACTURE PROBLEMS IN HYDRO-ELASTO-PLASTIC BODIES *1)

Tang Hansong2)
(*Beijing University of Aeronautics and Astronautics, Beijing*)

Abstract

A finite difference method is proposed for modeling wave motion and fracture phenomenon in hydro-elasto-plastic bodies. The method is a Godunov type approach, and it has second-order accuracy and captures shocks and fracture zones with high resolution. In the class of given wave systems the Riemann problems involved in the method have unique solutions, and the solutions can be obtained with efficient procedures. Numerical results are satisfactory in computations of Riemann problems and spallation in a steel plate.

1. Introduction

The study of higher-order accuracy and high resolution schemes for elastic and plastic wave problems is becoming a more important topic. Complex factors such as material behaviors make the investigation to be difficult. Recently, progress has been made by employing Godunov methods, c.f., [1,2,3]. In this paper, a new Godunov method will be proposed for modeling wave motion and fracture phenomenon in elasto-plastic media.

A hydro-elasto-plastic body is an elasto-plastic model with characters of solid and fluid phases[4]. The model describes transition between the two phases naturally as well as continuously, and it is often used in engineering problems such as explosion and high-velocity impact. Based on the standard MUSCL scheme

---

* Received January 6, 1998.

1) Supported by the National Natural Science Foundation of China and the Aeronautic Science Foundation of China.

2) Current address: School of Civil and Environmental Engineering, Georgia Institute of Technology, Atlanta, GA 30332, USA.

due to van Leer [5], a second-order scheme for gas-water-cavity systems has been developed[6], and it was applied to clarify certain puzzles in an experiment[7]. In the paper, solid phases are treated as a hydro-elasto-plastic body and the frame of the scheme in [6] will be employed.

The method proposed in this paper is second-order accurate, and it has high resolution for elastic and plastic shocks and describes onset and development of fractures in a simple way. The Riemann problems involved in the method have unique solutions and the solutions can be obtained with efficient procedures.

2. Governing Equation and Fracture Model

In Lagrangian coordinates, equations of motion for elasto-plastic media in plane strain may be written as the following system of conservation laws:

$$\frac{\partial U}{\partial t} + \frac{\partial F(U)}{\partial r} = 0, \tag{2.1a}$$

where

$$U = (V, u)^T, \qquad F(U) = (-u, P)^T, \tag{2.1b}$$

t is the time, r is the mass coordinates, $V = \rho_{ref.}/\rho$, $P = p/\rho_{ref.}$, and $\rho_{ref.}$, ρ, u , and p are a reference density, the density, the velocity, and the stress, respectively.

The constitutive equation for a hydro-elasto-plastic body may be written as

$$p = w(V) + \frac{4}{3}s(V_o, \tau_o, V). \tag{2.2a}$$

Here we use the Murnagham equation for the hydrostatic pressure:

$$w(V) = \frac{m}{\beta}\left(\left(\frac{V_a}{V}\right)^\beta - 1\right) + p_a \tag{2.2b}$$

and the Huber-Mises criterion for the shear stress:

$$s(V_o, \tau_o, V) = \begin{cases} \tau, & |\, \tau \,| < Y/2, \\ Y sign(\tau)/2, & |\, \tau \,| \geq Y/2 \end{cases} \tag{2.2c}$$

in which τ is determined by the Hooke's law:

$$\tau - \tau_o = -Gln\frac{V}{V_o}. \tag{2.2d}$$

In constitutive equation (2.2), G and Y are the modulus of rigidity and the yield stress, respectively, m and β are positive constants ($\beta \geq 1$), and subscripts a and o represent standard atmosphere conditions and initial states, respectively. In case of simple tension and compression, constitutive equation (2.2) can be rewritten as

$$p = \begin{cases} w(V) - 2Y/3, & p < p_1, \\ w(V) + 4\tau/3, & p_1 \leq p \leq p_2, \\ w(V) + 2Y/3, & p > p_2, \end{cases} \tag{2.3a}$$

where

$$p_1 = w(V_o e^{(2\tau_o - Y)/(2G)}) - \frac{2}{3}Y,$$
$$p_2 = w(V_o e^{(2\tau_o + Y)/(2G)}) + \frac{2}{3}Y. \tag{2.3b}$$

Here, subscripts 1 and 2 stand for the tension and the compression yield points, respectively.

Transient fracture will take place when tension is sufficiently large thus that the following criterion is satisfied:

$$p = p_v (< 0), \tag{2.4}$$

where subscript v indicates transient fracture. Assuming that a fracture zone is a vacuum and noticing that a solid phase can no longer sustain any tension at the place where it has cracked, we express (2.3a) as

$$p = max(p, \varphi p_v), \tag{2.5}$$

where $\varphi = 0, 1$, meaning the solid does and does not break in history, respectively. Besides, as a result of fatigue, fracture will also take place if the following is satisfied[8]:

$$\int_0^\delta \left(\frac{p_f - min(p, p_f)}{\mid p_f \mid}\right)^\lambda dt = K, \tag{2.6}$$

where p_f is the upper bound for onset of fatigue, δ is the time when the fracture occurs, and λ and K are constants. The above constitutive equation and fracture model have been applied in practice, e.g., [9].

3. Riemann Problem

3.1 Solution of the Riemann problem

Consider the Riemann problem for system (2.1) with the initial condition:

$$U_{t=0} = \begin{cases} H_l, & r < r_0, \\ H_r, & r > r_0, \end{cases} \tag{3.1}$$

where $H = (V, u)^T$, r_0 being a constant, and subscripts l and r representing the left and the right sides of r_0, respectively. In general, the solution to a Riemann problem for a hyperbolic system of conservation laws consists of centered waves connected by constant states. But its concrete form depends on the problem itself (e.g., [10,11,6]). Since constitutive equation (2.2) has yield points, after resolution of discontinuity (3.1) there may be a double-wave structure, comprised by an elastic and a plastic wave, at each side of r_0. The structure is either a double-shock or a double-rarefaction. When the following holds true:

$$u_l - u_r \leq \int_{\rho_l}^{\rho_v} \frac{c}{\rho} d\rho + \int_{\rho_r}^{\rho_v} \frac{c}{\rho} d\rho \tag{3.2}$$

a vacuum will occur in the resolution. Here, $c = \sqrt{\partial p/\partial \rho}$, being the sound speed. Criterion (3.2) corresponds to the case that $p \le p_v$. We will use centered waves, constant states, and vacuum zones to construct the solution to Riemann problem (2.1) and (3.1).

Resolution I If inequality (3.2) is not satisfied, the solution to Riemann problem (2.1) and (3.1) consists of constant states connected by (from the left to the right) a single- or a double-shock (or -rarefaction), a contact discontinuity, and a single- or a double-shock (or -rarefaction).

Resolution II If inequality (3.2) is satisfied, the solution to Riemann problem (2.1) and (3.1) consists of constant states connected by (from the left to the right) a single- or a double-shock (or -rarefaction), a vacuum, and a single- or double-shock (or -rarefaction).

First, we consider Resolution I. Let superscript $*$ represent resolved states besides r_0 and subscripts s stand for l or r.

1) $P^* \le P_1$. Now there is a double-rarefaction at side s. Within a rarefaction, the Riemann invariant is a constant along characteristics. As a result, for the elastic and the plastic rarefactions we have, respectively,

$$u_1 - u_s = \pm \int_{\rho_s}^{\rho_1} \frac{c}{\rho} d\rho, \qquad u^* - u_1 = \pm \int_{\rho_1}^{\rho^*} \frac{c}{\rho} d\rho, \tag{3.3}$$

which gives rise to

$$u^* - u_s = \pm \int_{\rho_s}^{\rho^*} \frac{c}{\rho} d\rho. \tag{3.4}$$

2) $P_1 < P^* \le P_s$. There is only an elastic rarefaction, and (3.4) still holds true.

3) $P_s < P^* \le P_2$. There is an elastic shock. From (2.1) the following Rankine-Hugoniot is derived:

$$\pm W_e(V^* - V_s) + (u^* - u_s) = 0, \tag{3.5a}$$

$$\pm W_e(u^* - u_s) - (P^* - P_s) = 0. \tag{3.5b}$$

Here W_e is the elastic shock speed in Lagrangian coordinates, and $\pm$ indicates the direction of propagation of the shock, positive and negative signs corresponding to the right and the left, respectively. (3.5) yields

$$u^* - u_s = \pm \frac{P^* - P_s}{W_e}, \tag{3.6a}$$

$$W_e = \sqrt{\frac{P^* - P_s}{V_s - V^*}}. \tag{3.6b}$$

4) $P_2 < P^* \le P_3$. Subscript 3 means the point where $(P_3 - P_2)/(V_3 - V_2) = (P_2 - P_s)/(V_2 - V_s)$. Now, a double-shock appears. From the R–H conditions for the elastic and the plastic shocks we have

$$u^* - u_s = \pm\left(\frac{P_2 - P_s}{W_e} + \frac{P^* - P_2}{W_p}\right). \tag{3.7a}$$

$$W_p = \sqrt{\frac{P^* - P_2}{V_2 - V^*}}. \tag{3.7b}$$

Here W_p is the plastic shock speed in Lagrangian coordinates.

5) $P^* > P_3$. Again, a steady shock, an elasto-plastic wave, will occur. By a discussion similar to 3), we have

$$u^* - u_s = \pm\frac{P^* - P_s}{W_{ep}}, \tag{3.8a}$$

$$W_{ep} = \sqrt{\frac{P^* - P_s}{V_s - V^*}}, \tag{3.8b}$$

where W_{ep} is the elasto-plastic shock speed in Lagrangian coordinates.

In view of above discussions, we conclude that in case of no vacuum state

$$u^* - u_s = \pm f(V_s, P_s, P^*), \tag{3.9a}$$

where

$$f(V_s, P_s, P^*) = \begin{cases} \int_{\rho_s}^{\rho^*} \frac{c}{\rho} d\rho, & P^* \le P_s, \\ \frac{P^* - P_s}{W_e}, & P_s < P^* \le P_2, \\ \frac{P_2 - P_s}{W_e} + \frac{P^* - P_2}{W_p}, & P_2 < P^* \le P_3, \\ \frac{P^* - P_s}{W_{ep}}, & P^* > P_3. \end{cases} \tag{3.9b}$$

Iteration is necessary for solving (3.9a). Eliminating u^* in (3.9a) gives rise to

$$f(V_l, P_l, P^*) + f(V_r, P_r, P^*) - (u_l - u_r) = 0, \tag{3.10}$$

which can be solved by the Newton method:

$$P^{(n+1)} = P^{(n)} - \left(\frac{F_1(P)}{dF_1(P)/dP}\right)^{(n)}, \tag{3.11a}$$

where

$$F_1(P) \equiv f(V_l, P_l, P) + f(V_r, P_r, P) - (u_l - u_r), \tag{3.11b}$$

$$P^{(0)} = P_v. \tag{3.11c}$$

In solving (3.10), V can also be determined by applying a Newton method to (2.3). Incorporating P^*, the limite of $P^{(n)}$, into (3.9a) and (2.3) gives u^* and V^*, respectively.

Second, we consider Resolution II. When there is a vacuum state, all above discussions hold true, but now

$$P^* = 0. \tag{3.12}$$

Consequently,

$$u^* = \pm f(V_s, P_s, 0) + u_s. \tag{3.13}$$

V^* is still determined by (2.3).

3.2 Existence, uniqueness, and convergence

Lemma. *$f(V_s, P_s, P)$ is continuous, and its first and second derivatives are positive and negative, respectively.*

Proof. Obviously, $f(V_s, P_s, P)$ is continuous within $(-\infty, P_s]$, $(P_s, P_2]$, $(P_2, P_3]$, and $(P_3, +\infty)$ and

$$\lim_{P\to P_s-0} f(V_s, P_s, P) = \lim_{P\to P_s+0} f(V_s, P_s, P) = 0, \tag{3.14a}$$

$$\lim_{P\to P_2-0} f(V_s, P_s, P) = \lim_{P\to P_2+0} f(V_s, P_s, P) = f(V_s, P_s, P_2). \tag{3.14b}$$

$$\lim_{P\to P_3-0} f(V_s, P_s, P) = \lim_{P\to P_3+0} f(V_s, P_s, P) = f(V_s, P_s, P_3). \tag{3.14c}$$

(3.9b) yields

$$\frac{df(V_s, P_s, P)}{dP} = \begin{cases} \frac{1}{C}, & P \le P_s, \\ \frac{1}{2}(\frac{1}{W_e} + \frac{W_e}{C^2}), & P_s < P \le P_2, \\ \frac{1}{2}(\frac{1}{W_p} + \frac{W_p}{C^2}), & P_2 < P \le P_3, \\ \frac{1}{2}(\frac{1}{W_{ep}} + \frac{W_{ep}}{C^2}), & P > P_3, \end{cases} \tag{3.15}$$

where $C \equiv \sqrt{-\partial P/\partial V}$, being the Lagrangian sound speed. Also, (3.9b) gives rise to

$$\frac{d^2 f(V_s, P_s, P)}{dP^2} =$$
$$\begin{cases} -\frac{\beta+1}{2C^3 V}, & P \le P_1, \\ -\frac{1}{2C^5}(\frac{m(\beta+1)V_a^\beta}{\rho_{ref.}V^{\beta+1}} + \frac{4G}{3\rho_{ref.}V^2}), & P_1 < P \le P_s, \\ -\frac{1}{2C^4}(\frac{(W_e^2 - C^2)^2}{2W_e^3(V_s - V)} + \frac{m(\beta+1)W_e V_a^\beta}{\rho_{ref.}C^2 V^{\beta+2}} + \frac{4GW_e}{3\rho_{ref.}C^2V^2}), & P_s < P \le P_2, \\ -\frac{1}{2C^4}(\frac{(W_p^2 - C^2)^2}{2W_p^3(V_s - V)} + \frac{(\beta+1)W_p}{V}), & P_2 < P \le P_3, \\ -\frac{1}{2C^4}(\frac{(W_{ep}^2 - C^2)^2}{2W_{ep}^3(V_s - V)} + \frac{(\beta+1)W_{ep}}{V}), & P > P_3, \end{cases} \tag{3.16}$$

From (3.15) and (3.16) it is readily seen that the Lemma holds true.

Theorem. (1) *The solution, as constructed in Resolutions I and II, to Riemann problem* (2.1) *and* (3.1) *exists uniquely.* (2) *In case of Resolution I, Newton method* (3.11) *converges to the solution.*

Proof. (1). First, consider Resolution I. Let

$$F_2(P) \equiv f(V_l, P_l, P) + f(V_r, P_r, P). \tag{3.17}$$

Since (3.2) does not hold, we have

$$u_l - u_r > \int_{\rho_l}^{\rho_v} \frac{c}{\rho} d\rho + \int_{\rho_r}^{\rho_v} \frac{c}{\rho} d\rho = F_2(P_v), \tag{3.18}$$

which is

$$F_1(P_v) < 0. \tag{3.19}$$

The definition of $F_1(P)$ yields

$$F_1(+\infty) = +\infty. \tag{3.20}$$

Also, it is known from the above Lemma that $F_1(P)$ is monotonically increasing. As a result, $F_1(P)$ passes zero point once and only once, or, (3.10) has a unique solution P^*. In view of (3.9a) and (2.3), the existence and uniqueness of P^* guarantees that u^* and V^* exist uniquely.

Second, consider Resolution II. Obviously, (3.12), (3.13), and (2.3) explicitly determine the existence and uniqueness of P^*, u^*, and V^*, respectively.

(2). Let (P_v, M) be an interval and M is sufficiently large such that $F_1(M) > 0$ and $P^* \in (P_v, M)$. From (3.19), (3.20), and the Lemma, we know that

1) $F_1(P_v)F_1(M) < 0$,
2) $dF_1(P)/dP \neq 0$,
3) $dF_1^2(P)/dP^2 < 0$,
4) $(F_1(P) \cdot dF_1^2(P)/dP^2)_{P=P_v} > 0$.

It can be proved that iteration (3.11) converges to its fixed point (e.g, [12]):

$$\lim_{n\to\infty} P^{(n)} = P^*. \tag{3.21}$$

The proof is completed.

4. Generalized Riemann Problem

Consider the following initial value problem:

$$U_{t=0} = \begin{cases} Q_l(r), & r < r_0, \\ Q_r(r), & r > r_0. \end{cases} \tag{4.1}$$

Here, $Q(r) = (V(r), u(r))^T$, $Q(r)$ being a linear function of r, and

$$\lim_{r\to r_0-0} Q_l(r) = H_l, \quad \lim_{r\to r_0+0} Q_r(r) = H_r. \tag{4.2}$$

We call initial value problem (2.1) and (4.1) the generalized Riemann problem of Riemann problem (2.1) and (3.1). We assume that the generalized Riemann problem has a solution with a same wave system as that of Riemann problem (2.1) and (3.1), and follow the way of van Leer [5] to derive time derivatives $(\partial u/\partial t)^*$ and $(\partial P/\partial t)^*$.

First, suppose the generalized Riemann problem has a solution with no vacuum state. When $P^* \le P_s$, (3.4) holds because of the above assumption. Differentiating (3.4) yields

$$\frac{D}{Dt}(u^* - u_s) = \pm\frac{D}{Dt}\int_{\rho_s}^{\rho^*}\frac{c}{\rho}d\rho. \tag{4.3}$$

With the aid of (2.1), it is derived from (4.3) that

$$(\frac{\partial u}{\partial t})^* \pm (-\frac{1}{C^*})(\frac{\partial P}{\partial t})^* = \pm C_s(\frac{\partial u}{\partial r})_s - (\frac{\partial P}{\partial r})_s, \quad P^* \le P_s. \tag{4.4}$$

By a similar way the following is obtained:

$$\begin{aligned}&(\frac{W_e^2}{2C^{*2}} + \frac{3}{2})(\frac{\partial u}{\partial t})^* \pm (-\frac{3W_e}{2C^{*2}} - \frac{1}{2W_e})(\frac{\partial P}{\partial t})^* \\ = \;& \pm(\frac{3W_e}{2} + \frac{C_s^2}{2W_e})(\frac{\partial u}{\partial r})_s - (\frac{W_e^2}{2C_s^2} + \frac{3}{2})(\frac{\partial P}{\partial r})_s, \quad P_s < P^* \le P_2.\end{aligned} \tag{4.5}$$

$$\begin{aligned}&(\frac{W_p^2}{2C^{*2}} + \frac{3}{2})(\frac{\partial u}{\partial t})^* \pm (-\frac{3W_p}{2C^{*2}} - \frac{1}{2W_p})(\frac{\partial P}{\partial t})^* \\ = \;& \pm(\frac{3W_e}{2} + \frac{C_s^2}{2W_e})(\frac{\partial u}{\partial r})_s - (\frac{W_e^2}{2C_s^2} + \frac{3}{2})(\frac{\partial P}{\partial r})_s, \quad P_2 < P^* \le P_3.\end{aligned} \tag{4.6}$$

$$\begin{aligned}&(\frac{W_{ep}^2}{2C^{*2}} + \frac{3}{2})(\frac{\partial u}{\partial t})^* \pm (-\frac{3W_{ep}}{2C^{*2}} - \frac{1}{2W_{ep}})(\frac{\partial P}{\partial t})^* \\ = \;& \pm(\frac{3W_{ep}}{2} + \frac{C_s^2}{2W_{ep}})(\frac{\partial u}{\partial r})_s - (\frac{W_{ep}^2}{2C_s^2} + \frac{3}{2})(\frac{\partial P}{\partial r})_s, \quad P^* > P_3.\end{aligned} \tag{4.7}$$

Two equations among (4.4)–(4.7), one for a right-moving wave and the other for a left-moving wave, make up a linear system for the time derivatives:

$$\begin{pmatrix} a_{11} & -a_{12} \\ a_{21} & a_{22}\end{pmatrix}\begin{pmatrix} \left(\dfrac{\partial u}{\partial t}\right)^* \\ \left(\dfrac{\partial P}{\partial t}\right)^*\end{pmatrix} = \begin{pmatrix} b_1 \\ b_2 \end{pmatrix}. \tag{4.8}$$

Here, a_{mk} and $b_m(m,k = 1,2)$ are given by (4.4)–(4.7), and it is readily seen that $a_{mk} > 0$. Consequently,

$$DET(a_{km}) = a_{11}a_{22} + a_{12}a_{21} > 0. \tag{4.9}$$

Then, we have the following conclusion.

Assertion Linear system (4.8) has a unique solution.

Second, suppose the generalized Riemann problem has a solution with a vacuum. Since there is no pressure on a solid surface adjacent to vacuum,

$$\left(\frac{\partial P}{\partial t}\right)^* = 0. \tag{4.10}$$

The velocity derivative of the surface can be obtained by incorporating (4.10) into (4.8):

$$(\frac{\partial u}{\partial t})^* = \frac{b_1}{a_{11}} \quad \text{and} \quad (\frac{\partial u}{\partial t})^* = \frac{b_2}{a_{21}}, \tag{4.11}$$

which correspond to the case that the surface is right or left to the vacuum, respectively.

5. Difference Scheme

Let $[t^n, t^{n+1}] \times [r_i, r_{i+1}]$ be a grid cell. Integrating (2.1) over the cell, using the Green law, and omitting the third-order terms give rise to a second-order formula:

$$\overline{V}^{n+1}_{i+1/2} = \overline{V}^n_{i+1/2} + \lambda^n_{i+1/2}(\langle u\rangle^n_{(i+1)-} - \langle u\rangle^n_{i+}). \tag{5.1a}$$

$$\overline{u}^{n+1}_{i+1/2} = \overline{u}^n_{i+1/2} - \lambda^n_{i+1/2}(\langle P\rangle^n_{(i+1)-} - \langle P\rangle^n_{i+}). \tag{5.1b}$$

Here

$$\langle u\rangle = u^* + \frac{1}{2}\left(\frac{\partial u}{\partial t}\right)^* \Delta t, \qquad \langle P\rangle = P^* + \frac{1}{2}\left(\frac{\partial P}{\partial t}\right)^* \Delta t, \tag{5.1c}$$

$\lambda^n_{i+1/2} = \Delta^n t/\Delta_{i+1/2}r$, and $\Delta^n t = t^{n+1} - t^n$, $\Delta_{i+1/2}r = r_{i+1} - r_i$, being the time step and the grid spacing, respectively. The grid spacing may not be uniform. RHS of (5.1c) is determined by solutions of a local Riemann problem and a local generalized Riemann problem as described in sections 3 and 4, respectively. The initial value for the two problems is

$$\overline{u}^n_{i\pm1/2} + \frac{\Delta^n_{i\pm1/2}u^*}{2}(r - r_{i\pm1/2}), \tag{5.2a}$$

$$\overline{P}^n_{i\pm1/2} + \frac{\Delta^n_{i\pm1/2}P^*}{2}(r - r_{i\pm1/2}), \tag{5.2b}$$

where $\Delta^n_{i+1/2}u^* = \langle u\rangle^{n-1}_{(i+1)-} - \langle u\rangle^{n-1}_{i+}$, $\Delta^n_{i+1/2}P^* = \langle P\rangle^{n-1}_{(i+1)-} - \langle P\rangle^{n-1}_{i+}$. Suppose that during time interval $[t^n, t^{n+1}]$, each slab experiences a simple tension or a simple compression process. As a result, (2.2) yields

$$\overline{P}^{n+1}_{i+1/2} = \begin{cases} \dfrac{1}{\rho_{ref.}}(w(\overline{V}^{n+1}_{i+1/2}) - \dfrac{2}{3}Y), & \overline{P}^{n+1}_{i+1/2} < P^{n+1}_{i+1/2,1}, \\ \dfrac{1}{\rho_{ref.}}(w(\overline{V}^{n+1}_{i+1/2}) + \dfrac{4}{3}\overline{\tau}^{n+1}_{i+1/2}), & P^{n+1}_{i+1/2,1} \le \overline{P}^{n+1}_{i+1/2} \le P^{n+1}_{i+1/2,2}, \\ \dfrac{1}{\rho_{ref.}}(w(\overline{V}^{n+1}_{i+1/2}) + \dfrac{2}{3}Y), & \overline{P}^{n+1}_{i+1/2} > P^{n+1}_{i+1/2,2}, \end{cases} \tag{5.3a}$$

$$\overline{\tau}^{n+1}_{i+1/2} = \overline{\tau}^{n}_{i+1/2} - Gln\frac{\overline{V}^{n+1}_{i+1/2}}{\overline{V}^{n}_{i+1/2}}, \tag{5.3b}$$

$$\begin{aligned} P^{n+1}_{i+1/2,1} &= \frac{1}{\rho_{ref.}}(w(\overline{V}^{n}_{i+1/2}e^{(2\overline{\tau}^{n}_{i+1/2}-Y)/(2G)}) - \frac{2}{3}Y), \\ P^{n+1}_{i+1/2,2} &= \frac{1}{\rho_{ref.}}(w(\overline{V}^{n}_{i+1/2}e^{(2\overline{\tau}^{n}_{i+1/2}+Y)/(2G)}) + \frac{2}{3}Y). \end{aligned} \tag{5.3c}$$

We assume a fracture can and only can take place at a grid node. Whether transient fracture happens or not at node i depends on resolved states of local initial discontinuity (5.2). The following criterion determines if fracture of fatigue occurs or not there:

$$\Sigma_n(\frac{P_f - min((\overline{P}^{n}_{i-1/2} + \overline{P}^{n}_{i+1/2})/2, P_f)}{\mid P_f \mid})^{\lambda}\Delta^n t = K. \tag{5.4}$$

The location of fracture is tracked by

$$x^{n+1}_{i\pm} = x^{n}_{i\pm} + \langle u\rangle^{n}_{i\pm}\Delta^n t. \tag{5.5}$$

Formulas (5.1)—(5.5) are the difference scheme for hydro-elasto-plastic bodies. The scheme keeps the features of van Leer's MUSCL scheme [5] designed for continuous gases, that is, it has second-order accuracy and high resolution. But, it is also able to describe onset and development of fracture. In (5.2), let $\Delta^{n}_{i+1/2}u^* = \Delta^{n}_{i+1/2}P^* = 0$, the scheme becomes the first-order accurate. To prevent numerical oscillations, the monotonicity preserving algorithm (101) in [5] is necessary. Furthermore, to reduce numerical error due to appearance of vacuum states, the following algorithm of lower bound of density is adopted [6]:

$$\Delta^{n}_{i+1/2}u^* = min\left(\Delta^{n}_{i+1/2}u^*, \overline{V}^{n}_{i+1/2}\left(1 - \frac{\overline{V}^{n}_{i+1/2}}{V_v}\right)\frac{\Delta_{i+1/2}r}{\Delta^{n-1}t}\right). \tag{5.6}$$

Also, some restrictions on the time step are needed. Waves within a slab should not intersect with each other:

$$\Delta^n t \leq \frac{CFL\Delta_{i+1/2}r}{2max(\mid W^{n}_{i+} \mid, \mid W^{n}_{(i+1)-} \mid)}, \tag{5.7}$$

where W^n_i is the speed of a shock or that of the front of a rarefaction, $CFL \leq 1$. Zone tangling should be avoided ($\Delta^{n}_{i+1/2}u^* < 0$):

$$\Delta^n t \leq -\frac{x^{n}_{(i+1)-} - x^{n}_{i+}}{\Delta^{n}_{i+1/2}u^*}. \tag{5.8}$$

When there is a fracture between two slabs, the two slabs should not overlap with each other ($\langle u\rangle^{n}_{i-} > \langle u\rangle^{n}_{i+}$):

$$\Delta^n t \leq \frac{x^{n}_{i+} - x^{n}_{i-}}{\langle u\rangle^{n}_{i-} - \langle u\rangle^{n}_{i+}}. \tag{5.9}$$

In problems with oscillating stress, $\Delta^n t$ is also restricted by frequency of the oscillation.

6. Numerical Examples

6.1 Riemann problems

We compute the following two Riemann problems in steel media:

$$I \begin{cases} \rho = 7802.32kg/m^3, u = 50m/s, \ p = 10^8 Pa, & x < 0, \\ \rho = 7846.85kg/m^3, u = -50m/s, \ p = 2 \times 10^9 Pa, & x > 0, \end{cases} \quad (6.1)$$

$$II \begin{cases} \rho = 8046.83kg/m^3, u = -1000m/s, \ p = 8 \times 10^9 Pa, & x < 0, \\ \rho = 7881.14kg/m^3, u = 1000m/s, \ p = 3 \times 10^9 Pa, & x > 0. \end{cases} \quad (6.2)$$

With reference to [9] and [13], we use the following properties for the steel:

$$\begin{aligned} &\rho_a = 7800kg/m^3, \ m = 2.225 \times 10^{11} Pa, \ \beta = 3.7, \\ &G = 0.853 \times 10^{11} Pa, \ Y = 0.00979 \times 10^{11} Pa, \ p_v = -0.2 \times 10^{11} Pa, \\ &p_f = -0.019292 \times 10^{11} Pa, \ \lambda = 1.33, \ K = 3.35 \times 10^{-6} s. \end{aligned} \quad (6.3)$$

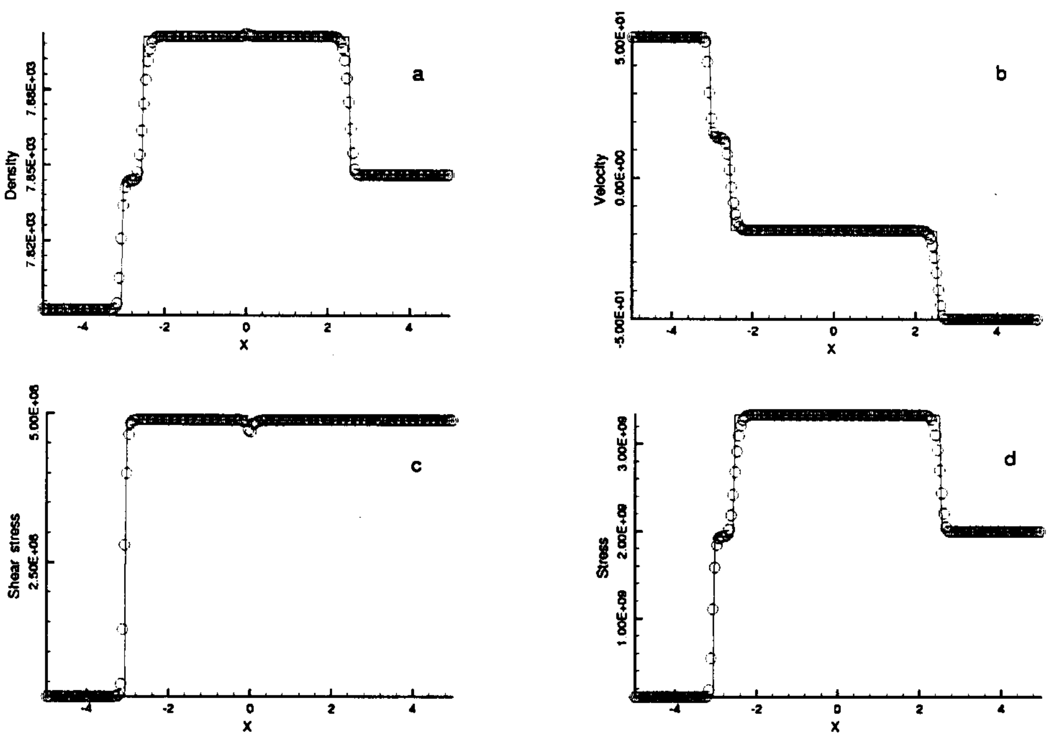

Fig. 1. Riemann problem I. Slab number=200, time step=150, CFL=1.
Solid lines – exact solutions, circles – numerical solutions.

Problem I is a collision between two steel plates. As a consequence of the collision, an elastic and a plastic shock move to the left, and an elastic shock propagates to the right. Problem II corresponds a transient fracture in a plate. The fracture results in a left-moving elastic and a left-moving plastic rarefaction, a right-moving elastic rarefaction, and a vacuum lying between the left- and right-moving rarefactions. The numerical results are given in Figs. 1 and 2. Comparing the numerical solutions with the corresponding exact solutions, we see that the proposed scheme clearly resolves the elastic and plastic waves and the fracture. The scheme presents no obvious oscillations near shocks and its resolution for them is similar to that of the Godunov scheme in [1].

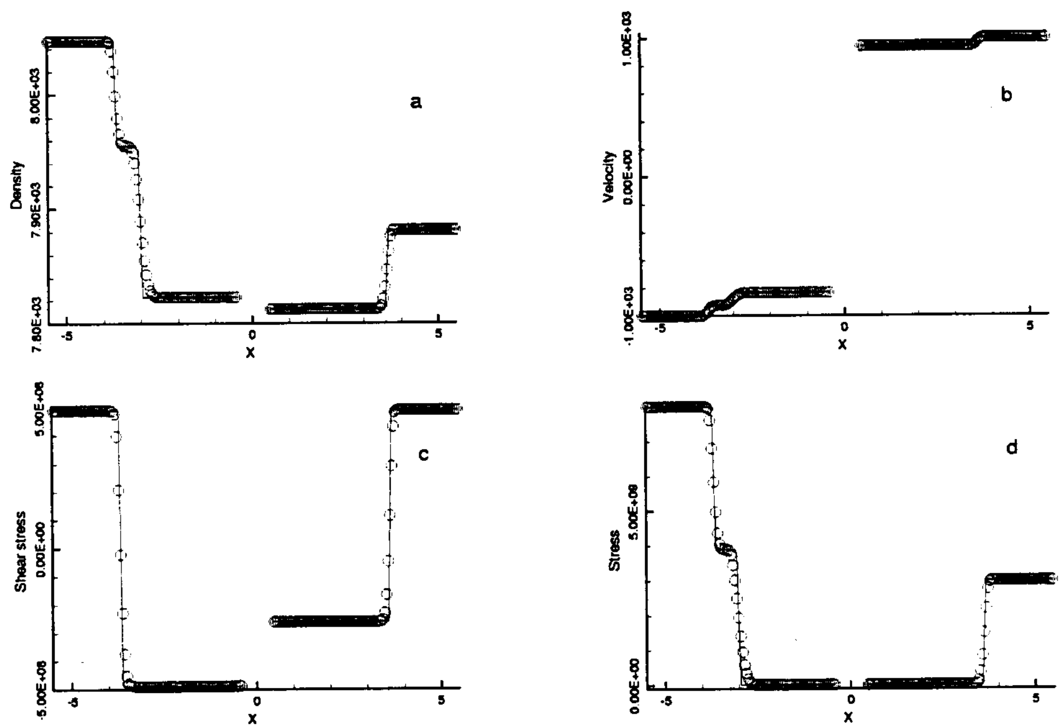

Fig. 2. Riemann problem II. Slab number=200, time step=160, CFL=1. Solid lines – exact solutions, circles – numerical solutions.

6.2 Spallation due to explosion

A layer of dynamite 1 m in thickness and a steel plate 1 m in thickness are placed at the left and the right sides of $x = 0$, respectively. After the dynamite is ignited at its left side, the gaseous product resulting from the explosion flies freely towards the left and a blast propagates to the right. As the blast reaches the plate, a shock is generated in the plate, and the computation starts. In the computation, the density of the dynamite is $1600kg/m^3$, the ratio of specific heats of the gaseous product is 1.4, and the blast speed is $7667m/s$. The gaseous product is calculated using the method in [6]. Again, properties of the plate is set as (6.3). Initially, $\rho = \rho_a$, $u = 0$, $p = p_a$ in the plate. On the left side of the product and the right side of the plate, $p = 0$ and $p = p_a$ are respectively imposed as boundary conditions.

The numerical results are presented in Fig. 3. The computation shows that our Godunov method clearly resolves the shock (Fig. 3a). Since the strength of the shock is much stronger than the yield stress, the elastic precursor is not observed in the figure, and it is actually a plastic wave. The method also predicts a phenomenon of spallation due to fatigue (Fig. 3b). The computed process of spallation is similar to that described in [9]; some time after the shock reflects at the right side of the plate, a spallation sheet is produced, and spallation zones propagate from the sheet to the left (Fig. 3c).

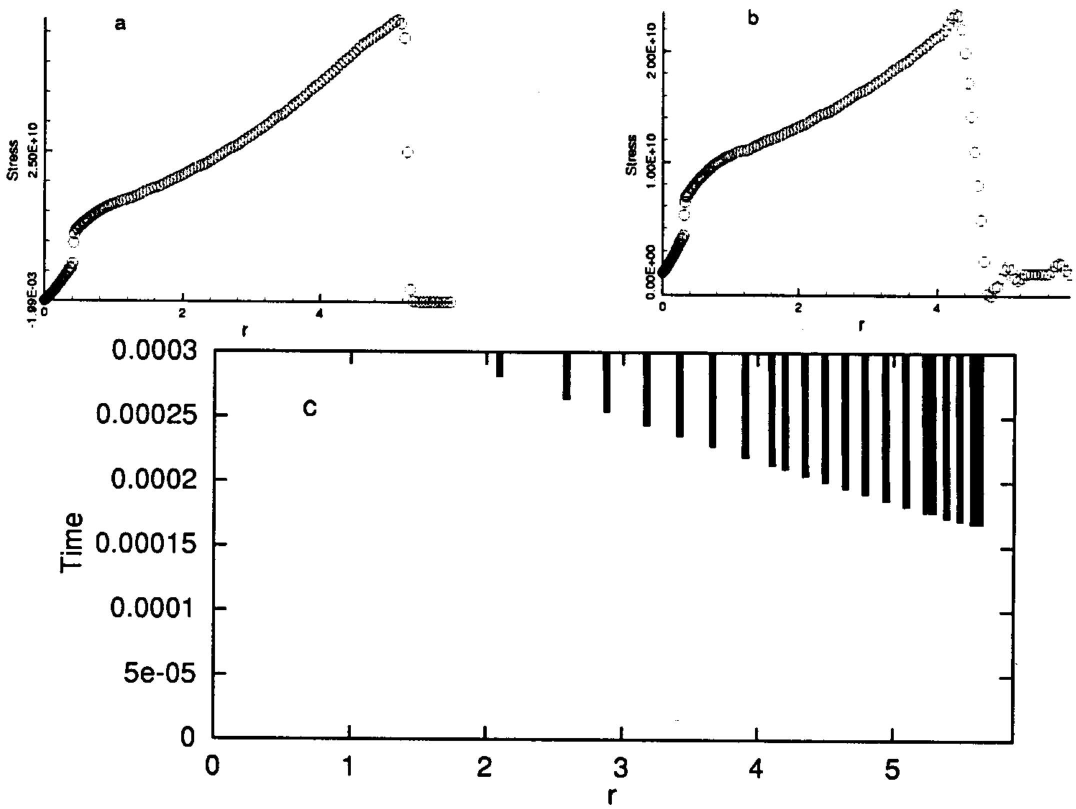

Fig. 3. The spallation problem. The left and the right sides of the plate are located at $r = 1, 5.875$ ($\rho_{ref.} = 1600 kg/m^3$), respectively. Slab number is 200(product) × 100(steel), and CFL=1. a) Stress distribution at $t = 1.3 \times 10^{-4} s$. The shock is approaching the right side of the plate. b) Stress distribution at $t = 1.9 \times 10^{-4} s$. The shock has reflected at the right side of the plate. c) Spallation zones. Spallation zones propagate to the left.

7. Concluding Remarks

We have proposed a second-order Godunov method for wave and fracture problems in hydro-elasto-plastic bodies. The method is useful in investigating mechanism of high-velocity impact as well as that of its consequent fracture. Also, it can be combined with the scheme presented in [6] to formulate a numerical algorithm for gas-water-solid systems with cavitation and spallation. A further study about the method could be its extension to multiple spatial dimensions.

References

[1] J. Trangenstei and P. Colella. A higher-order Godunov method for modelling finite deformation in elastic-plastic solids, *Comm. Pure Appl. Math.*, **44**(1991), 41–100

[2] F. Wang, J. G. Glimm, J. W. Grove, and B. J. Plohr. A conservative Eulerian numerical scheme for elastoplasticity and application to plate impact problems, *Impact Comput. Sci. Engrg.*, **5**(1993), 285–308

[3] G. H. Miller and E. G. Puckett. A high-order Godunov method for multiple condensed phases, *J. Comput. Phys.*, **128**(1996), 134–164

[4] Z. M. Zheng, Hydro-elasto-plastic body, *Chinese Encyclopedia, Mechanics*, Encyclopedia Press (Beijing), 1985, 343–345 (Chinese)

[5] B. van Leer. Towards the ultimate conservative difference scheme, V. A second-order sequel to Godunov's method, *J. Comput. Phys.*, **32**(1979), 101–136

[6] H. S. Tang and D. Huang. A second-order accurate capturing scheme for 1D inviscid flows of gas and water with vacuum zones, *J. Comput. Phys.*, **128**(1996), 301–318

[7] H. S. Tang. Numerical study of cavitation phenomenon in water shock tube, *J. Hydrodynamics*, Ser. A, **12**(1997), 175–180 (Chinese)

[8] F. R. Tuler and M. B. Butcher, A criterion for the time dependence of dynamic fracture, *Int. J. Fra. Mech.*, **4**(1968), 431-437

[9] C. H. Chu, Y. C. Li, and X. J. Wang, Numerical analysis of steel plate's spallation due to explosion, *Appl. Math. and Mech.*, **2**(1981), 353–376 (Chinese)

[10] P. Lax. Hyperbolic systems of conservation laws, *Comm. Pure Appl. Math.*, **10**(1957), 537–566

[11] T. P. Liu and J. A. Smoller. On the vacuum state for the isentropic gas dynamics equations, *Adv. in Appl. Math.*, **1**(1980), 345–359

[12] Z. H. Zhao, Y. D., Zhang, and R. X. Li, *Computing Matrixes and Solving Euqations*, 2ed ed., High education Press (Beijing), 1979 (Chinese)

[13] Z. P. Duan, C. Q. Shuan, D. G. Yuang, N. Q. Tian, and Y. Cu, Experimental and theoretical studies on dynamical features of metals under high ratio of strain, *Progress in Mech.*, **10**(1980), 1–16 (Chinese)